



Study of the topographic and optical properties of gold metal nanomaterial's prepared with three pulses laser (300,500,700)

**Atyaf Sarhan Farhan
Alrubaie**

University of AL-Qadisiyah, Department of physics, IRAQ
atyaf.s.farhan@qu.edu.iq

ABSTRACT

The gold nanoparticles were prepared. With ionic water laser ablation using an (Nd: Yag) laser with a wavelength of 532 nm and energy (90mJ) using three different laser pulses (300, 500, and 700), deionized liquid water was used. The crystalline nature has been studied through an X-ray diffraction device, and the results showed that gold nanomaterial has the cubic structure (FCC); As for the surface, terrain prepared. It was studied using an atomic force microscope. It was found that the increase in the number of laser pulses led to the rise in the large nanoparticles resulting from the agglomeration of small nanoparticles, thus increasing the average size of the NPS. As for the optical properties of colloidal gold nanoparticles, they were studied using the absorption spectra at wavelength range (300-1100) nanometer where an increase in absorbance was observed with a decrease in transmittance and an increase in the number of laser pulses, as well as a reduction of the value of the light energy gap.

Keywords:

Gold nanoparticle, Double distilled and deionized water, the topographic, optical properties

Introduction:

Nanotechnology is a new strategy in many applications, including engineering, medical, agricultural and even military [1]. This method is possible because of the technique's reliance on Nanoscale-sized particles. Structure, device, and system manufacturing, manipulation, and application via nanometer-scale control of form and size is a fast developing discipline. The nano in nanotechnology comes from the Greek word for "very small" (meaning dwarf). The length, width, and thickness all come in at 100 nm or less. Their distinctive properties stem from a combination of their microscopic size, chemical make-up, and surface structure. The physical features motivate innovation and boost productivity in research, opening up avenues for the creation of industrial, medicinal, agricultural, and technical applications [2]. Nanoparticles are present in the environment in general, such as water, air and soil, and they are either naturally or from

unnatural sources of pollution that include industrial and combustion processes and the various processes for the production of nanoparticles [3].

Material and experimental Spectrophotometer work principle

The spectrometer is utilized in biological and chemical laboratories to determine the level of the many factors such as nitrates, phosphates, sulphates, silicates, sugar, heavy elements and dyes, etc., as this device has a wide range of analytical uses. A spectrophotometer is a method for determining the reflectivity or absorbance of sample wavelengths. This method depends on that all the compounds reflect the light by a particular value of wavelengths. This technique measures the level of absorbed photons by the sample if the photon passes inside it, and the examination obtains the concentration of the material.



Figure (1) : Show Spectrophotometer apparatus

Optical constant

1-Absorption Coefficient

Beer-Lambert law is laws in optics that determine the relationship between material properties and light absorption. Lambert's law confirms that the light absorption is depended on the light path length, while Beer's law confirm that the light absorption is depended on the level of the absorbing particles in the sample; the Beer-Lambert law is included that the light intensity that pass through the material reduce depending on the level and thickness of the material within the certain wavelength, when the concentration of the material was more, the absorbed light become more with decreasing of the transient beam energy logarithmically. The law showed a logarithmic correlation between the light transmittance and the sample absorption coefficient, and the light that moves through the sample and mathematical relationship as following [4]:

$$\log (I / I_0) = -\epsilon [J]L \dots\dots\dots (7),$$

ϵ : molecular absorption coefficient
 I: light intensity
 I₀: collision severity
 [J]: molar level

Absorbance, The term absorbance in physics refers to the process of absorbing light. Still, usually, some of the incident light particles are scattered, so the term light extinction or light attenuation may be used instead of absorbance, as the absorbance is proportional to the thickness of the sample and the concentration of absorbent particles in the sample, either As for the unit of and after the Reform. The equation (7), we get [4]:

$$\epsilon = 2.303 A/t \dots\dots\dots (8)$$

The structural and optical properties
(A)X-ray diffraction device

XRD is an analytical method used to determine the crystalline material and give data cell dimensions. The tested material is homogenized, finely ground, and the bulk composition is estimated.



Figure (2): show X-ray Diffraction Device

(B)Atomic force microscope Principle

The atomic force microscope's cantilever, which is used to scan over a sample's surface, is very sharp. A deflection towards the surface

occurs when the tip is close to the surface due to the attractive force between the material surface and the tip. After the cantilever's tip makes contact with the specimen surface, the

instrument is forced to deflect away from the surface. Deflections towards something away from the laser beam are measured. The laser beam is altered after being reflected. Using a position-sensitive photodiode to detect the shifts. The PSPD also keeps track of the cantilever deflection caused by the AFM tip as

it moves over the sample surface. Scanning the sample area results in an AFM image. PSPD discovers that the deflection of a cantilever responds to both an increase and reduction in the sample's surface. The AFM creates a precise surface map [9].

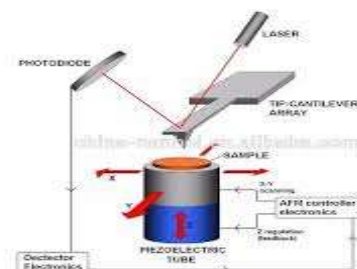


Figure show (4): X-ray Diffraction Device

(C) Field emission Scanning electron microscope

FESEM provides topographic and DATA at magnification (10-300,000) x, with depth of field. Compared to scanning electron microscopy (SEM), SEM field emission (FESEM) results in sharper and less electrostatic distortion images with a spatial resolution of 1 1/2 nm – (3-6) times better. Its other features can examine smaller contamination regions at accelerating electron voltages compatible with energy dispersive spectroscopy (EDS). Electrons with a low kinetic energy may explore further into a substance without damaging it. Low-voltage, high-quality photos that may be used as samples. Voltages from 0.5

to 30 kilovolts (kV) are sped up. An in-lens FESEM is used for ultra-zoom imaging. In terms of practical use, it has a wide variety of potential applications. Cross-sectional studies of semiconductor devices for inspecting gate and gate oxides, layer thickness, and building details. Coatings are now applied in uniform thickness, and their settings are more precise. Microcontamination, feature geometry, and the operational concept of scale component composition. More spatial resolution and less sample charge and damage are made possible by the field emission cathode in the electron pistol of a scanning electron microscope. We also provide in-lens FESEM [10] for situations that need the maximum possible magnification

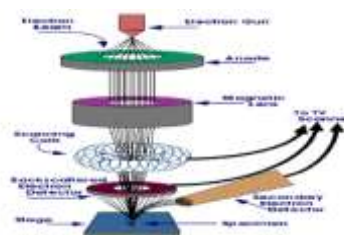


Figure show (5) shows FESEM Device [10]

Experimental

The nanomaterial was prepared by bringing the sample to the gold metal, where it would be polished and washed, then Distilled water to remove suspended impurities and then put into a quartz cell. It is placed in a solution of

DDDW in an amount of 2 millilitres. Set up the analytical row in DDDW. (Q-Switch Nd-YAG) pulse. Energy (90mJ) has been used; Pulse duration and laser pulse repetition rate were ten ns and six hertz, respectively. The number of used pulses was (300, 500 and 700). Next,

the PVA membranes were prepared by dissolution. (0.5) a gram of PVA powder was stirred in (10) millilitres of Double distilled and deionized water at (50 degrees) mixed for (120) minutes to produce a viscous solution. After you finish ruining. (2) mL of Au NPs suspension. It was added to 10 millilitres of PVA solution. Samples were left to dry at (25) C for seven days. The diffraction pattern was used to analyze crystal structure. He then used the AFM to analyze sample topography, study the linear optical properties of Au NPs, and fast scanning electron microscopy.

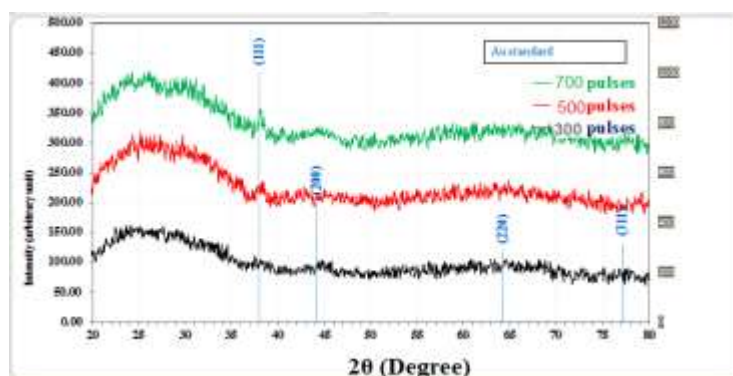
Conclusion:

XRD results show a clear and sharp peak with Dominant peaks. Au NPS is ready. With a polycrystalline structure (JCPDS No. 96-901-3038). Figure (6) shows the X-ray diffraction of nanomaterial's prepared from pure gold. By ionic water by laser ablation with three laser

pulses 300, 500 and 700 pulses, as it was observed to be polymorphic and sharp. Peaks in crystal levels (111), (200), (220) and (311) peaks at two and a half values (38.0105 °, 44.177 °, 65.255 °, 78.156 °), in contrast, approximately, where the maximum percentage of crystalline levels is at the level (111), Figure (6) shows X-ray diffraction of Au Thin NPs in Double distilled and deionized water. There was a decrease in the intensity value with the offset of the angle value as the random material approaches as a result of the laser ablation process that corresponds to the ref [11], indicating the presence of gold particles implanted with the Fcc structure into the region in agreement with the EXAFS result. All the tests were conducted in the Islamic Republic of Iran, Kashan University The average particle size was measured by Debbie Shearer's equation (11), as shown in Table (1).

Table (1): X-ray diffraction for Au NP colloid at 300 ,500,700 pulse

pulse	2θ (Deg.)	FWHM (Deg.)	d _{hkl} Exp.(Å)	G.S (nm)	d _{hkl} Std.(Å)	Phase	hkl	card No.
300	38.1501	1.1613	2.3571	7.2	2.3654	Cub. Au	(111)	96-901-3038
500	38.2199	0.9773	2.3529	8.6	2.3654	Cub. Au	(111)	96-901-3038
700	38.1152	0.8726	2.3591	9.6	2.3654	Cub. Au	(111)	96-901-3038



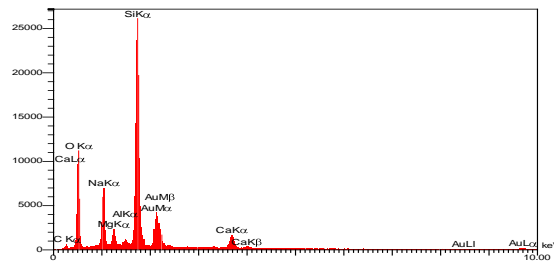
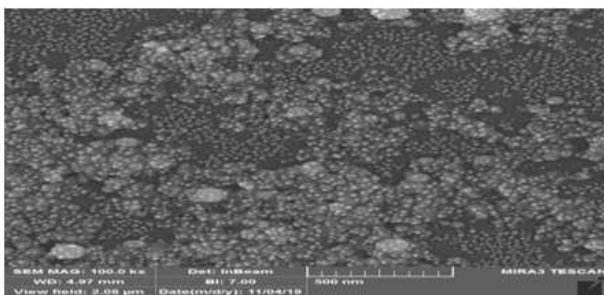


Figure (6): X-Ray diffraction for Au NPs thin film by 300,500,700 pulse

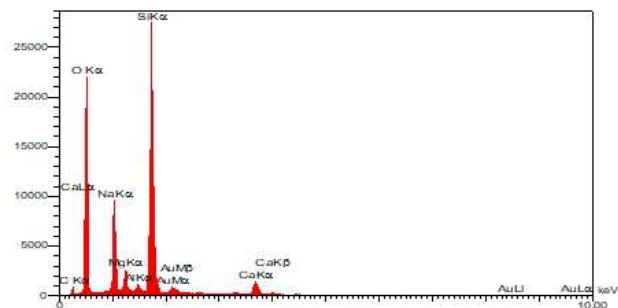
(D) FSEM image and EDX diagram:

Particle size, shape and morphological were studied by FE-SEM equipped. FE-SEM images of Au nanoparticle thin films deposited on the glass Substrate for different ablation pulses are presented in Figure (7-a), Figure (8-a), Figure (9-a) from figures it have been shown that the formation of Au nanoparticles with various sizes. The gold nanoparticles have a spherical shape. The Aggregation is not grossly and with increasing The ablation pulses that results in increasing the size of the spherical Of Au nanoparticles. These Au nanoparticles were used to in the light scattering layer In photoanodes Also, it can be observed from figures that the grain Boundaries were

observed for spherical truncated nanoparticles; their limits can be understood in terms of surface thermodynamics .and attributed to ionic interaction between specimens. Fig.(7-b),(8-b), (9-b) shows the energy dispersion analysis for Au nanoparticles.EDX presents results, there is major peak singles correspond to Si content on SEM diffraction, and Cu, C singles are formed; also, it is known that gold shows energy intensities at 2keV and 2.6 keV.The EDX of Au nanoparticles This indicates that besides of high Au peak intensity, there is a small amounts of other particles located onto gold surface were also found during the samples preparation



(a)



(b)

Figure show (7) FE-SEM image and EDX diagram for Au nanoparticles deposited on glass substrate at ablation 300 pulse

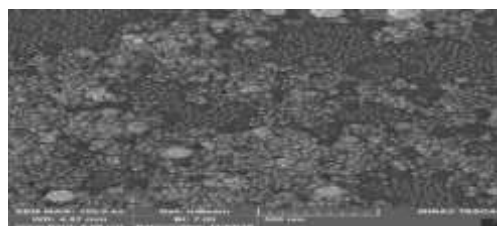


Figure show (8) FE-SEM image and EDX diagram for Au nanoparticles deposited on glass substrate at ablation 500 pulse

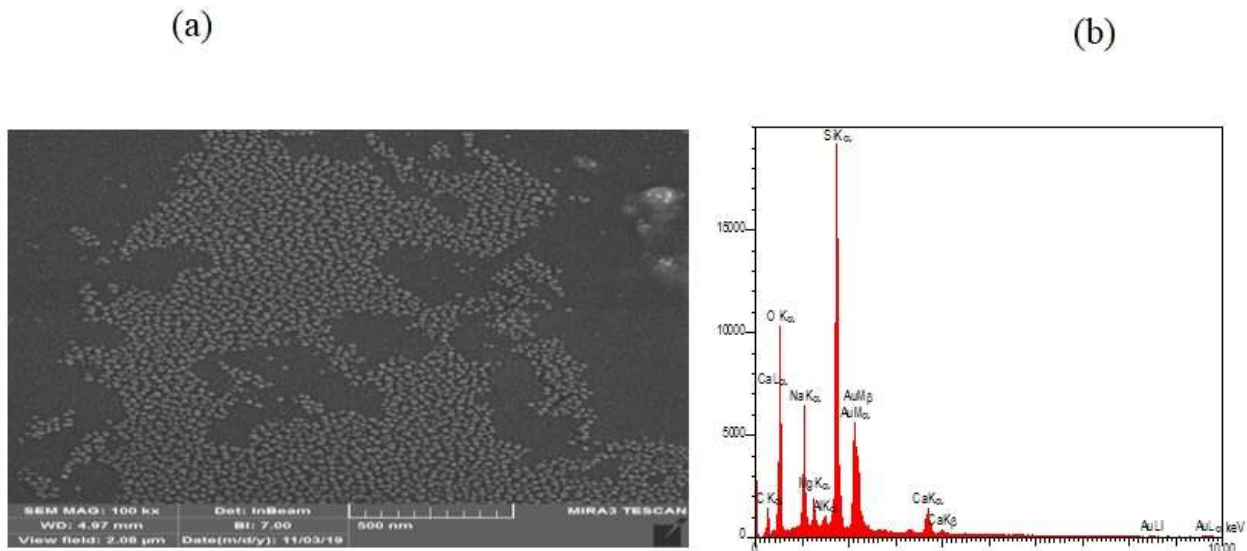


Figure show (9) FE-SEM and EDX diagram image for Au nanoparticles deposited on glass substrate at ablation 700 pulse

(E)Atomic Force Microscopy (AFM)

The grain size (grain diameter) Atomic Force Microscopy AFM.Au characterized gold nanoparticles' average roughness with different ablation pulses (300, 500, 700) nm. The topographical synthesized by laser ablation are shown in Fig (10-a, b, c), respectively. It was evident from the table (2) that the high Pulsed laser ablation leading into the disappearing of small Au- NPs and growing of Au-NPs due to the agglomeration of small particles into big ones and, correspondingly, the average grain size of Au NPs get to increase. Indeed the grain size increases from

1.188 nm to 27.63 nm when pulsed The laser increases from 300-700, respectively. The average roughness and RMS increase with them; on the other hand, the roughness increases from 3.574 to 9.125 nm.

Furthermore, RMS increases from 4.009nm to 9.885nm, respectively, when pulsed laser increases. These results are due to structure enhancement. Also, it can be noticed from the table that the values of the roughness and RMS is very closed to each other, and this is given an indication is the films is very homogenous in preparation

Table (2) (RMS) and AV. Diameter Au NPs at (E=90mj, λ=532nm)

pulsed	Ave. grain size (nm)	Ave. Roughness (nm)	RMS (nm)
300	1.188	3.574	4.009
500	22.13	5.539	6.885
700	27.63	9.125	9.885

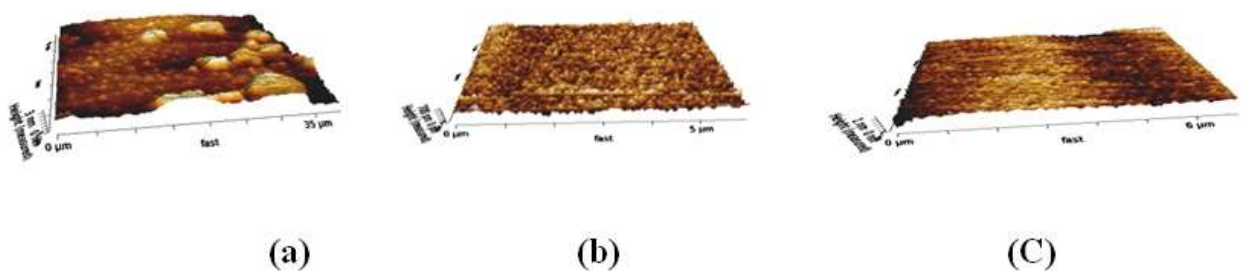


Figure show (10): Atomic Force Microscopy (AFM) for 300, 500, 700 pulses

Optical Properties of Au nanoparticles:

(1) Absorption Spectrum

Figure (11) showed UV- absorption wavelength of Au-Nanoparticles by laser ablation method at many laser ablation. The absorbance of Au nanoparticles is very weak. Besides, the absorbance resonance peak of gold nanoparticles has obviously red-shifted. In general, it is found that all the films have the same behaviour with a wavelength that is decreasing of absorption value with increasing of wavelength while increases with increasing of the pulsed laser from 300 pulses to 700 pulses indicating that the absorption process is carried out by increases the Au nanoparticles concentration in the suspension and increases the absorption of the thin films. Also., The estimated peaks of 520–540 nm are suspended on Au-nanoparticles production [12, 13]. The maximum wavelength means a slight redshift

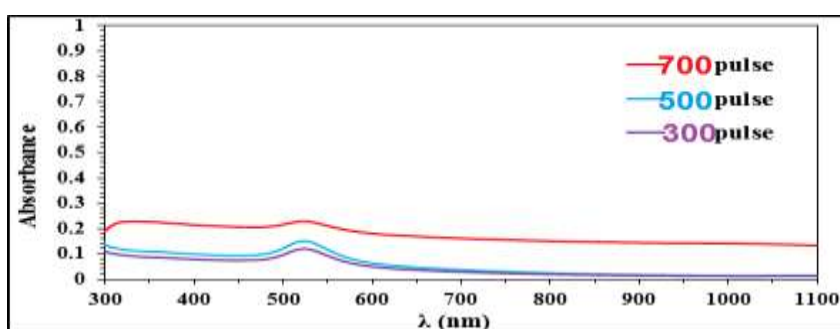


Figure (11): UV-VIS absorption spectra of the Au nanoparticles at different laser pulses

(2) The Transmission spectrum:

Figure (12) demonstrate the spectral optical transmittance as (300–1100) nm for au nanoparticles at different laser pulses. From the figure, In general, the transmission spectrum's behaviour is opposite of the absorption spectrum. It is found that all the films have the same action with a wavelength that is increasing of transmission with increasing of wavelength while decreases .with increasing of the pulsed laser from 300 pulses to 700 pulses indicating that the absorption process is carried out by increases the Au in the suspension and increases the absorption of the thin films with increasing of the laser pulses, which leading high absorption, the films

from (520) nm to (540) nm. According to the Mie theory, such a shift is due to the size reduction of particles [14]. The level of Au-nanoparticles By increasing the ablation pulsed from 300 to 700 pulsed, the particle size inside the Nanofluid decreased from cm to nm. The peak intensity depends on the concentration of the Au-NPs in suspension and increases with increasing particle concentration action or ablation pulse. Despite the broad spectrum, this peak arose from a SPR of the Au-NPs Nanomaterial's showed significant properties separate from the material due to the large surface region, spatial confinement and high Surface energy. The laser is absorbed by NPs due to low reflection and strong absorption. Gold NP showed high absorption near to (520) nm and not showed the bulk material due to the surface Plasmon oscillation modes of conduction electrons in NPs [15].

were highly transmittance in the visible wavelength region with an average transmittance in excess of 90%. This is probably ascribed to the increase of particle sizes and surface roughness. The maximum transmission observed For Au-NPs prepared at 200 pulses was almost (90%), while for increasing the pulsed to the 600, the transmittance decrease to equal (60%). The behavior of the transmission is the opposite of absorption. Also, it can be observed that the transmission spectra have a negative peak which is occurred around 520-540 nm for All samples and is redshifted to 520 nm and 540 nm for samples 3 and 4 respectively. This peak is due to surface plasmonic resonance (SPR)

absorption of Au nanoparticles. The redshift of the corresponding wavelengths of SPR confirms that is increasing particle size

redshifts the SPR wavelength .and also increases the intensity.

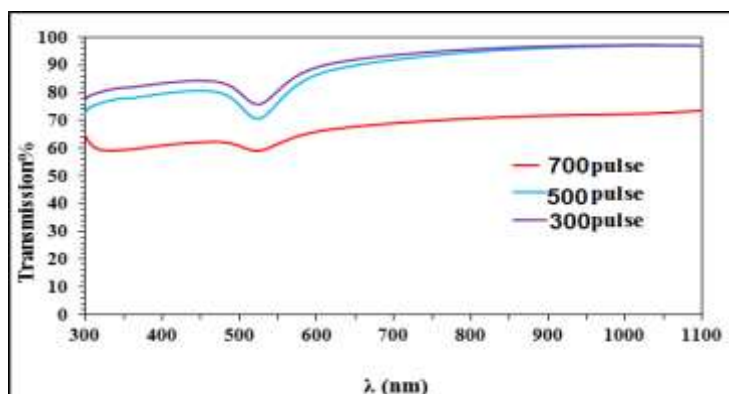


Figure (12): The transmittance spectrum (%T) Au Nanocomposite film prepared by laser ablation method in different pulsed laser

(3)The energy Gap:

Using the absorption coefficient data in Tauc model bandgap energy of Au, the bandgap means that the energy distance between the conduction and the valence is considered a key optical factor that showed the optical transitions. The smaller the bandgap, have high the electric conductive. Figure (14) revealed the variation measured from UV-absorption with the photon. Energy The optical band gap are determined by the extrapolation of the best fit line between bandgap and photon energy. Figure 5 showed that the value of optical band gap comes out to be and gap energy reduces with raise the level of Au NPS in the solution, as shown in Figure. The energy gaps of Au nanoparticles are depended on Au level or size. Au nanoparticles are responsible for producing localized electronic states that demonstrate all the optical and electrical properties wherever decrease the energy leading to changes in the band gap. When the optical band gap decreases, the disorder degree of the films become high and leads to changes in the polymer [16].

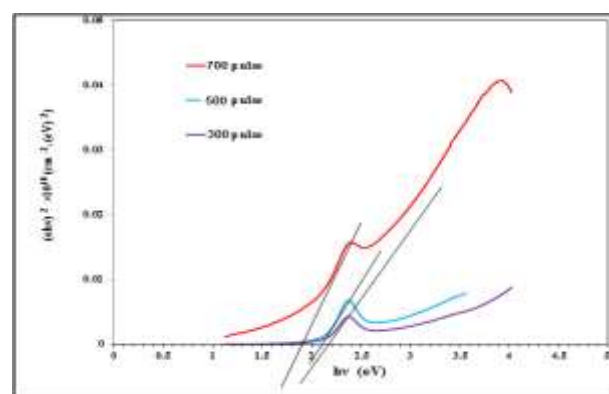


Figure (13) energy gap of the Au nanoparticles at different laser pulses

References

1. **Mohamed A.ShakerPhD, Mona I.ShaabanPhD (2017).** Synthesis of silver nanoparticles with antimicrobial and anti-adherence activities against multidrug-resistant isolates from *Acinetobacter baumannii* Sciences Volume, August 2017, Pages 291-297
2. **MHS Ahmida, NHS Ahmida(2017).** Introduction to nanotechnology: definition, terms, occurrence and applications in environment - Libyan International ..., 2017 - journal.limu.edu.ly
3. **Mohmed H. S. Ahmida, Nagwa H. S. Ahmida and Aziza A. Ahmeida.** Introduction to nanotechnology:

- definition, terms, occurrence and applications in environment.
Citation DOI:
[10.21502/limuj.003.02.2017](https://doi.org/10.21502/limuj.003.02.2017) LIMUJ, Volume 2, PP 12-26 2017
4. **Maha .R.(2012)**. Characteristics of Some Metals Nanoparticles Thin Film Prepared by PLD Technique, Thesis, College of Science for Women, University of Babylon.
 5. **Eman. K. (2017)**. Study the Effect of Multi-Layers Deposition (TiO₂/ZnO:Se/CdS:Se) on the Performance of Laser Textured (P-Type) Silicon, Thesis, Collage of Science for Women at the University of Babylon.
 6. **Mahdi, Z. F., & Ali, A. A. (2012)**. Investigation of nonlinear optical properties for laser dyes-doped polymer thin film. Iraqi journal of physics, 10(19), 54-69.
 7. Suh I.-K., Ohta H., Waseda Y., "High-temperature thermal expansion of six metallic elements measured by dilatation method and X-ray diffraction Locality: synthetic Sample: at T = 676 K", Journal of Materials Science 23, 757-760 (1988)
 8. [8]C. F. Bohren and D. R. Huffman, Absorption and Scattering of Light by Small Particles Wiley, New York, 1983, 217
 9. **Miller, J. C., & Haglund, R. F. (Eds.). (1998)**. Laser ablation and desorption (Vol. 30, p. 29). New York: Academic Press.
 10. **van Roon JL1, van Aelst AC, Schroën CG, Tramper J, Beeftink HH. (2005)**. Field-emission scanning electron microscopy analysis of morphology and enzyme distribution within an industrial bio catalytic particle. Scanning.;27 (4):181-
 11. **C. F. Bohren and D. R. Huffman**, Absorption and Scattering of Light by Small Particles Wiley, New York, 1983, 217
 12. **Atyaf Sarhan Farhan(2020)**, Preparation and Study the Linear and Non-Linear Optical Properties for Colloidal AuNPs Using Nd:YAG and Their effect in Human Blood Health.
 13. **Shih C.M., Y.-T. Shieh, and Y.-K. Twu, (2009)**. Preparation of gold nanoparticles and
 14. nanoparticles using chitosan suspensions," Carbohydrate Polymers, vol. 78, no. 2, pp. 309 315.
 15. **Abdelaziz, M. (2011)**. Cerium (III) doping effects on optical and thermal properties of PVA films, Physica B: Condensed Matter Volume 406, Issues 6–7, Pages 1300-130.
 16. **Abdlzhra, A. F., Abdllatief, I. A., & Alabodi, E. E. L. (2016)**. Preparation and Characterization of Silver Nanoparticles and Study Their effect on the Electrical Conductivity of the Polymer Blend (Poly vinyle acitet. Pectin, poly Aniline). Ibn AL-Haitham Journal For Pure and Applied Science, 29(3), 379-389
 17. **M.Abdelaziz,PhysicaB406,1300(2011)**